DEBONDING OF INTERFACIAL CRACKS IN SANDWICH BEAMS

E. E. Gdoutos
School of Engineering
Democritus University of Thrace
GR-671 00 Xanthi, Greece

Summary. The debonding facing failure of a cantilever beam made of aluminum facings and PVC foam cores is studied by linear elastic fracture mechanics. Results for the stress and displacement fields are obtained using finite elements. It was obtained that for weak interfaces debonding grows along the interface, while for strong interfaces, crack kinks into the core. After a small initial curved depth h_∞ the crack becomes parallel to the interface. It was obtained that h_∞ is inversely proportional to the modulus of elasticity of the core material and independent of the core thickness.

Introduction

Facesheet debonding may develop during fabrication of sandwich panels or may be caused by external loading such as impact. Debonding reduces the stiffness of the structure and makes it susceptible to buckling under in-plane compression. Facesheet/core debonding failures and interfacial cracking have been studied by many investigators over the last two decades by means of experimental, numerical and analytical methods [1-9]. The mechanical and failure behaviour of composite sandwich beams was studied by Gdoutos and Daniel in a series of publications [10-17].

Beams with aluminum honeycomb cores showed some premature debonding failure in some cases due to the very small bonded area of the honeycomb cross section. The effect of debonding in double cantilever beam specimens made of aluminum facesheets and PVC foam cores (Fig. 1) was studied by Gdoutos and Balopoulos [18]. The analysis used linear elastic fracture mechanics of interfacial cracks in conjunction with finite elements.

In the present work we consider a sandwich double cantilever beam (*DCB*) specimen made of aluminum facing and foam core with initial debonding in the form of an interfacial crack (Fig. 1). The growth behavior of the interfacial crack is studied by a finite element analysis coupled with failure criteria.
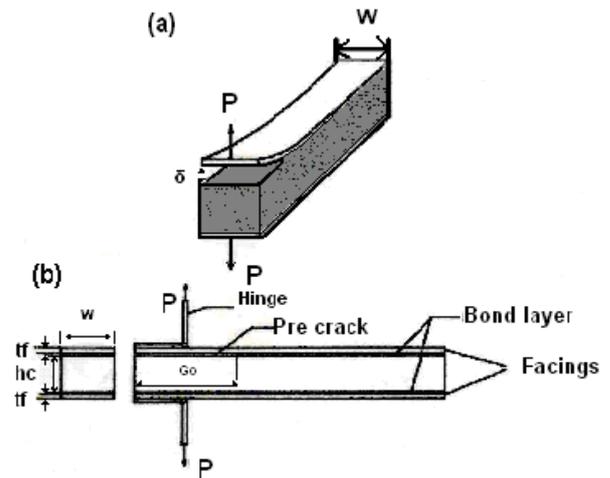

Fig. 1: Double cantilever sandwich beam specimen.

Debonding of sandwich beams

The strain energy release rate for interfacial crack growth is given by

$$G_{\text{int}} = \frac{1}{2}\left[\frac{1}{\overline{E_1}} + \frac{1}{\overline{E_2}}\right]\left(K_{\text{I}}^2 + K_{\text{II}}^2\right) \qquad (1)$$

where $\overline{E_j} = E_j/\left(1 - v_j^2\right)$ for plane strain, and $\overline{E_j} = E_j$ for plane stress, and for crack growth in a monolithic elastic material by

$$G_{\text{vol}} = \frac{K_{\text{I}}^2 + K_{\text{II}}^2}{\overline{E}} \qquad (2)$$

The interfacial crack may propagate along the interface or kink into one of the

adjoining materials. The angle of initial crack propagation, Ω, is given, according to the maximum tangential (hoop) stress criterion, by:

$$\Omega = 2\tan^{-1}\left(\frac{\sqrt{1+8\left(K_{\mathrm{II}}/K_{\mathrm{I}}\right)^2}-1}{4\,K_{\mathrm{II}}/K_{\mathrm{I}}}\right) \qquad (3)$$

Kinking of the interfacial crack into the core occurs when the following inequality is satisfied:

$$\left(\frac{\max\limits_{\Omega} G}{G_{\mathrm{I,cr}}}\right)_{\mathrm{core}} > \left(\frac{G}{G_{\mathrm{cr}}(\gamma)}\right)_{\mathrm{int}} \qquad (4)$$

The critical strain energy release rate for the core material in mode I, $G_{I,cr}$, and the critical interfacial strain energy release rate, $G_{cr}(\gamma)$, as function of mode mixity, are determined experimentally. They are characteristic parameters of the core and the interface, respectively. Values of $G_{Int,cr}$ and $G_{I,cr}$ are shown in Table 1. On the other hand, the values of energy release rate for crack growth in the core and along the interface depend on the applied loads and the geometry of the sandwich plate, and are determined numerically.

Table 1 Values of $G_{Int,cr}$ and $G_{I,cr}$ for various core materials

Materials	$G_{Int,cr}$ (Nmm/mm^2)	$G_{I,cr}$ (Nmm/mm^2)
Divinycell H60	0.28	0.10
Divinycell H80	0.45	0.22
Divinycell H100	0.78	0.30
Divinycell H250	1.55	1.00

We consider a sandwich double cantilever beam (DCB) specimen of length 152.4 mm (6 in) and width 25.4 mm (1 in) loaded by a concentrated load at a distance 25.4 mm (1 in) from its end (Fig. 1). The beam is made of aluminum 2024 T3 facings of thickness 1 mm and a PVC foam (Divinycell H) core of thickness 25.4 mm (1 in). The core is bonded to the facings by of epoxy adhesive of thickness 0.3 mm. Four different PVC core materials, H60, H80, H100, and H 250, were studied. An interfacial crack of length 51.1 mm (2 in.) is introduced between the core and the adhesive at the loaded end of the specimen. Propagation of the interfacial crack is studied under condition of plane strain.
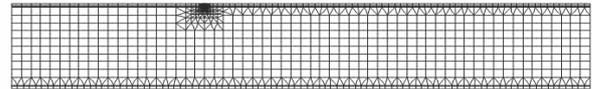

Fig. 2: Initial meshing.

The model of the sandwich DCB specimen is shown in Fig. 2. It is composed of seven topological regions. Each region is divided into regular and transition sub-regions. Sub-region boundaries are then subdivided into segments of appropriate number and proportions, and meshing is done automatically by boundary extrapolation, using Q8 and T6 elements for regular and transition sub-regions, respectively. The initial model contains 1501 elements (986 Q8 and 515 T6), of which 282 discretize the upper face, 114 the upper layer of adhesive, 97 the lower layer of adhesive, 97 the lower facing and 911 the core.

For the prediction of the crack trajectory we use the interface toughness values for normal adhesion (Table 1). It is obtained that first the interfacial crack kinks into the core and then curves back toward the interface (Fig. 3). For intermediate values of the distance x from the crack tip (3 mm< x <30 mm), we obtain the following results:

• the crack after a small depth h_∞ becomes parallel to the interface (Fig. 3)
• $K_{\mathrm{I,int}}$, $K_{\mathrm{II,int}}$, and $K_{\mathrm{I,core}}$ vary linearly with the distance x from the crack tip, and
• G_{int} and G_{core} vary linearly with x and are almost independent of the core properties.
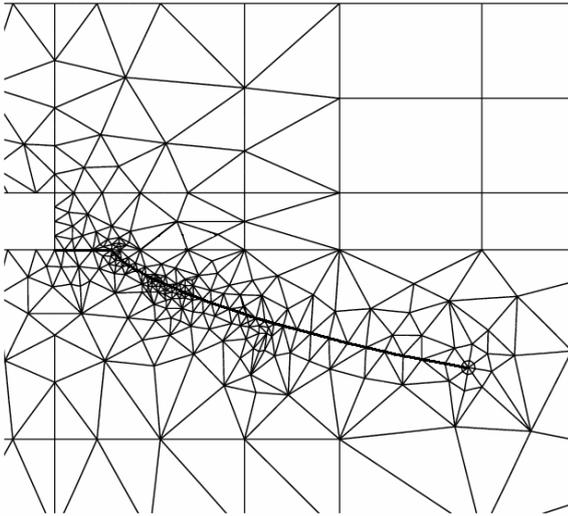
Fig. 3: Initial crack path trajectory.

Regarding the sub-interfacial crack propagation into the core we obtain that the crack becomes parallel to the interface at a constant depth h_∞. An explanation of the constant value of h_∞ and the linear variation of stress intensity factors with the distance from the crack tip x can be obtained by noting that the debonded part of the specimen (above the crack) can be considered as a thin cantilever beam ($l/d \sim 25$), elastically supported by the foam core, and subjected to a dominant bending moment varying linearly with x and to a relatively small (constant) shear force. Thus, the near-tip stress field is linearly proportional to x and, hence, the crack propagates in a self-similar manner parallel to the interface. The strain energy release rate can be determined by differentiating the work of the applied load with respect to the distance from the crack tip and is constant during crack propagation. Values of h_∞ for various core materials are shown in Table 2.

The core stiffness appears to be the main factor that influences the value of the asymptotic depth h_∞. Indeed, it can be obtained from Table 2 that the product $E\,h_\infty$ is almost constant and equal to 60 N/mm for the three PVC foam materials H60, H80 and

H250. For H100 it takes the value 70 N/mm. Thus, the depth h_∞ is inversely proportional to the modulus of elasticity of the core material.

Table 2. Values of critical distance h_∞

	$\overline{E}$ (GPa)	h_∞ (mm)	$\overline{E}h_\infty$ (N/mm)
H 60	0.059	1.01	59.6
H 80	0.087	0.70	60.9
H100	0.107	0.65	69.6
H 250	0.308	0.20	61.6

Under such conditions and for a critical applied load, debonding propagates along the interface only when the adhesion between the interface and the core is weak. Otherwise, the crack kinks into the core and after a small initial curved path it propagates parallel to the interface at a depth. The value of h_∞ is inversely proportional to the modulus of elasticity of the core. This behavior is independent of the core thickness, which is an order of magnitude larger than the thickness of the facing and the adhesive. Away from boundary effects (e.g., concentrated loads, beam supports, crack kinking, etc.) both stress intensity factors and strain energy release rate can be approximated as linear functions of the crack length.

Conclusions

An investigation of the debonding of the facing from the core in sandwich structures under a concentrated load was undertaken. When the applied load reaches a critical applied load, debonding propagates along the interface only when the adhesion between the interface and the core is weak. Otherwise, the crack kinks into the core and after a small initial curved path it propagates parallel to the interface at a depth h_∞. The value of h_∞ is inversely proportional to the modulus of elasticity of the core. Away from boundary effects (e.g., concentrated loads, beam supports, crack kinking, etc.) both stress

intensity factors and strain energy release rate can be approximated as linear functions of the crack length.

References

1. Prasad S, Carlsson LA (1994) Debonding and crack kinking in foam core sandwich beams. Analysis of fracture specimens. Eng Fract Mech 47(6): 813-824

2. Prasad S, Carlsson LA (1994) Debonding and crack kinking in foam core sandwich beams. Experimental investigation. Eng Fract Mech 47(6): 825

3. Grau DL, Qiu XS, Sankar BV (2006) Relation between interfacial fracture toughness and mode mixity in honeycomb core sandwich composites. J Sand Struct Mat 8(3): 187-203

4. Minakuchi S, Okabe Y, Takeda, N (2007) Real-time detection of debonding between honeycomb core and facesheet using small diameter FBG sensorembedded in adhesive layer. J Sand Struct Mat9 (1): 9-33

5. Berggreen C, Simonsen BC, Borum KK (2007) Experimental and numerical study of interface crackpropagation in foam-cored sandwich beams. J Comp Mat 41(4): 493-520

6. Jakobsen J, Bozhevolnaya E, and Thomsen OT (2007) New peel stopper concept for sandwich structures. Comp Sci Tech 67: 3378-3385

7. Aviles F, Carlsson LA (2008) Analysis of the sandwich DCB specimen for debond characterization. Eng Fract Mech 75(2): 153-168

8. Østergaard RC, Sørensen BF, Brøndsted P (2007) Measurement of interface fracture toughness ofsandwich structures under mixed mode loadings. J Sand Struct Mat 9: 445-466

9. Berggreen C, Simonsen BC, Borum KK (2007) Experimental and numerical study of interface crackpropagation in foam-cored sandwich beams. J Comp Mats 41: 493-520

10. Daniel IM, Gdoutos EE, Abot JL, Wang KA (2001) Core failure modes in composite sandwich beams. ASME, 2001, IMECE, AD-Vol. 65/AMD-Vol. 249: 293-303

11. Gdoutos EE., Daniel IM, Wang KA, Abot JL (2001) Nonlinear behavior of composite sandwich beams under three-point bending. Exp Mech 41(2): 182-188

12. Daniel IM, Gdoutos EE, Wang KA (2002) Failure of composite sandwich beams. Adv Comp Lett 11(2): 49-57

13. Daniel IM, Gdoutos EE, Wang KA, Abot JL (2002) Failure modes of composite sandwich beams. Int J Dam Mech 11: 309-334

14. Gdoutos EE., Daniel IM, Wang KA (2002) Indentation failure in composite sandwich structures. Exp Mech (42): 426-431

15. Abot JL, Daniel IM, Gdoutos EE (2002) Contact law for composite sandwich beams. J Sand Struct Mater (4): 157-173

16. Gdoutos EE., Daniel IM, Wang KA, Abot JL (2003) Compression facing wrinkling of composite sandwich structures. Mech Mater (35): 511-522

17.Daniel IM, Gdoutos EE, Abot JL, Wang KA (2003) Deformation and failure of composite sandwich structures. J Thermopl Comp Mater (16): 345-364

18 Gdoutos EE, Balopoulos V (2008) Kinking of interfacial cracks in sandwich beams. Proc Eighth Int Conf Sand Struct (ICSS8), Porto, Portugal